ELSEVIER

Physica B 316–317 (2002) 62–68

PHYSICA B

www.elsevier.com/locate/physb

Electron–phonon interactions in HTSC cuprates

T. Egami[a,*], J.-H. Chung[a], R.J. McQueeney[b], M. Yethiraj[c], H.A. Mook[c], C. Frost[d], Y. Petrov[e,1], F. Dogan[f], Y. Inamura[g], M. Arai[g], S. Tajima[h], Y. Endoh[i]

[a] *Department of Materials Science and Engineering and Laboratory for Research on the Structure of Matter LRSM, University of Pennsylvania, 3231 Walnut Street, Philadelphia, PA 19104-6272, USA*
[b] *Los Alamos National Laboratory, Los Alamos, NM 87545, USA*
[c] *Oak Ridge National Laboratory, Oak Ridge, TN 37831, USA*
[d] *Rutherford Appleton Laboratory, Didcot, OX11 0QX, UK*
[e] *Department of Physics and Astronomy, University of Pennsylvania, Philadelphia, PA 19104, USA*
[f] *Department of Materials Science and Engineering, University of Washington, Seattle, WA 98195, USA*
[g] *Institute of Materials Structure Science, KEK, Tsukuba 305, Japan*
[h] *Superconductivity Research Laboratory, International Superconductivity Technology Center, Tokyo 135-0062, Japan*
[i] *Institute for Materials Research, Tohoku University, Sendai 980, Japan*

Abstract

Phonons have been generally considered to be irrelevant to the high-temperature superconductivity in the cuprates. However, such a bias is usually based upon the assumption of conventional electron–phonon coupling, while in the cuprates the coupling can be rather unconventional because of strong electron correlation. We present the results of our recent measurements of phonon dispersion in $YBa_2Cu_3O_{6+x}$ by inelastic neutron scattering. These suggest certain phonon modes interact strongly with electrons and are closely involved in the superconductivity phenomenon with possible contribution to pairing.

Keywords: High-temperature superconductivity; Neutron scattering; Electron–phonon coupling

1. Introduction

The phonon mechanism was discarded early in the study of high-temperature superconductivity (HTSC). This is because the superconductive critical temperature in excess of 100 K appears to be too high for the BCS mechanism, the isotope effect is very weak, there is no indication of strong electron–phonon coupling in the normal state transport properties, and because the attractive phonon mechanism for pairing tends to cancel the repulsive magnetic mechanism. But this judgment to exclude the phonon mechanism may have been too premature; it is based on the conventional electron–phonon coupling, while the electron–phonon coupling in strongly correlated systems can be very different. Theories predict that it is strongly dependent on the momentum, energy and the phonon eigenvector. In particular it is predicted that the Cu–O bond-stretching LO mode interacts strongly with charge [1]. In addition the effect of spins and complex structures such as the

*Corresponding author. Tel.: +1-215-898-5138; fax: +1+215-573-2128.
E-mail address: egami@seas.upenn.edu (T. Egami).
[1] Present address: Gatsby Neuroscience Computational Unit, University College London, London WC1N 3AR, UK.

0921-4526/02/$ - see front matter
PII: S0921-4526(02)00426-X

spin/charge stripe structure must be considered before any intelligent judgment can be made.

In this paper, we describe the results of our recent inelastic neutron scattering measurements on single crystals of $YBa_2Cu_3O_{6+x}$ that demonstrate the unusual nature of electron–phonon interaction in this compound [2,3]. Measurements were made using the time-of-flight spectrometer MAPS of the ISIS facility of the Rutherford-Appleton Laboratory, as well as the triple-axis-spectrometer HB-2 and HB-3 at the HFIR of the Oak Ridge National Lab. We found that the dispersion of the Cu–O bond-stretching modes is strongly anisotropic in the CuO_2 plane due to anisotropic dielectric screening, suggesting significant anisotropy in the underlying electronic structure. The results are compatible with the spin/charge stripe model. The LO modes appear to interact strongly with electrons, in particular toward the zone edge, and may be in resonance forming the vibronic state. The phonon intensities show anomalous dependences on composition and temperature, and in the case of optimally doped $YBa_2Cu_3O_{6.95}$ the temperature dependence is directly related to the superconductive order parameter. The results on the underdoped samples indicate that they are made of nano-scale regions of optimally doped and undoped states. These findings challenge the present theories on the origin of HTSC and suggest that the possible involvement of the electron–phonon coupling in the HTSC mechanism has to be taken seriously. It is even possible that the phonon is the missing link in the HTSC theory.

2. Phonon dispersion measured by neutron scattering

The phonon dispersion is usually determined with the triple-axis-spectrometer which gives the one-dimensional scan, for instance over energy at a fixed $\boldsymbol{Q}$, of the dynamical structure factor, $S(\boldsymbol{Q},\omega)$. Here $\boldsymbol{Q}$ is the momentum transfer and ω is the energy transfer. With MAPS one obtains $S(\boldsymbol{Q},\omega)$ in three-dimensions (energy and two axes of momenta), allowing parallel, more efficient, determination of many phonon branches in one measurement. MAPS is equipped with a large number (~ 700) of position-sensitive ^{3}He neutron detectors that cover $16\,m^2$ with 2-dimensional 1.5×10^5 pixels. It produces a large data set, typically 1 GB per measurement. Using the data on vanadium as a reference, the raw data were converted into $S(\boldsymbol{Q},\omega)$ by the M-slice program. Even after the processing the data size is over 250 MB. Since the data set is so large it takes a very long time to examine the whole three-dimensional data space. In order to visualize the three-dimensional data more effectively M-slice yields various two-dimensional cuts, projected on the other two axes. As an example a constant energy cut 41 meV (integrated from 40 to 42 meV), projected on the $h-k$ plane, is given as Fig. 1. Here the momentum $\boldsymbol{Q}$ is represented in reciprocal lattice units (h, k, l). Since the sample is twinned, we used a provisional lattice constant of 3.84 Å to represent a/b. The sample was placed in a closed cycle helium refrigerator with the a/b-axis in the vertical position and the c-axis rotated away from the beam by 49°. This setting brings the l index close to zero around $\hbar\omega = 50$ meV at $\boldsymbol{Q} = (3,0,0)$. The data were taken at $T = 7$ K. Magnetic resonance peaks are seen at (0.5, $\pm$0.5, 0). Another cut, along $k = 0$ (integrated from $k = -0.1$ to 0.1), is presented in Fig. 2 as the $h-\omega$ projection. In this case the data were taken at $T = 110$ K ($T_C = 93$ K). Phonon dispersions are determined by peak-fitting to the 1-dimensional slices, typically the energy scan at a fixed $\boldsymbol{Q}$. The layered nature of the HTSC cuprate greatly simplified the interpretation of the results. In Figs. 1 and 2 actually the index l is also varying, but the l-dependence is generally weak because of the layered structure, and is neglected for the moment in the present analysis.

A close examination of the data in Fig. 2 allowed us to determine the phonon dispersions of the Cu–O bond-stretching phonons. In this projection since the phonon momentum, $\boldsymbol{q} = \boldsymbol{Q}-\boldsymbol{K}$, where $\boldsymbol{K}$ is the reciprocal lattice vector, is parallel to $\boldsymbol{Q}$, only the longitudinal (LO) phonons are seen, because the neutron scattering intensity is proportional to $(\boldsymbol{Q}\cdot\boldsymbol{\varepsilon})^2$, where $\boldsymbol{\varepsilon}$ is the phonon polarization vector. In order to see the transverse phonons (TO) another cut was made along the

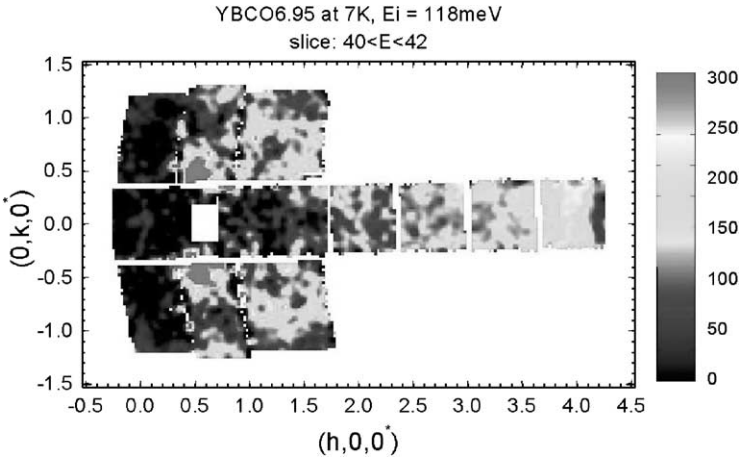

Fig. 1. A constant-energy cut of $S(\boldsymbol{Q},\omega)$ of $YBa_2Cu_3O_{6.95}$ at 41 meV at $T = 7$ K. The magnetic resonance peaks are seen at (0.5, $\pm$0.5, 0).

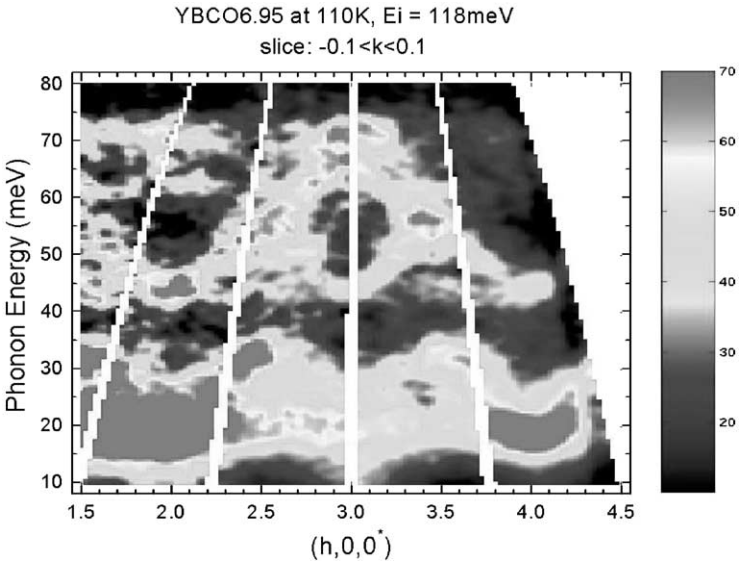

Fig. 2. $S(\boldsymbol{Q},\omega)$ of $YBa_2Cu_3O_{6.95}$ at $T = 110$ K cut at $k = 0$. In order to see the phonon dispersion better the data were divided by Q^2 after subtracting the multi-phonon background (about 40% of the total). The Cu–O bond-stretching phonon modes are seen in the energy range from 55 to 72 meV.

k-axis including the ***K*** point, where ***q*** is nearly perpendicular to ***Q***. In Fig. 2, near $\boldsymbol{Q} = (3, 0, 0)$ we noted there are two high-energy LO branches, one around 72 meV and the other around 67 meV. Interestingly the maximum of each branch was shifted slightly away from (3, 0, 0). The one at 72 meV has a maximum at (3.02, 0, 0), suggesting that the real lattice constant is 3.82 Å, very close to *a*. The other has a maximum at (2.96, 0, 0), yielding the lattice constant of 3.88 Å, identified as *b*. Thus, because of the orthorhombicity and difference in the energy by 3 meV, we were able to identify the branches along ***a*** and ***b***, even though the sample was twinned. This identification and

frequencies are in excellent agreement with the Raman data on an untwinned sample [4]. We then made a k-cut at $h = 3.05$, where only the TO modes are seen. Surprisingly it is nearly dispersionless up to $k \sim 0.25$, the limit of our measurement because of the vertical angle range of the detector coverage. Fig. 3 shows the cuts at $h =$ 3.05 and 2.95.

The h-cut at $k = 0$ and two k-cuts at $h = 3.02$ and 2.96 yielded the phonon dispersion as shown in Fig. 4. Here the difference between a and b has been corrected. Note that the branch denoted as B_{3g} at the zone center, with the polarization along

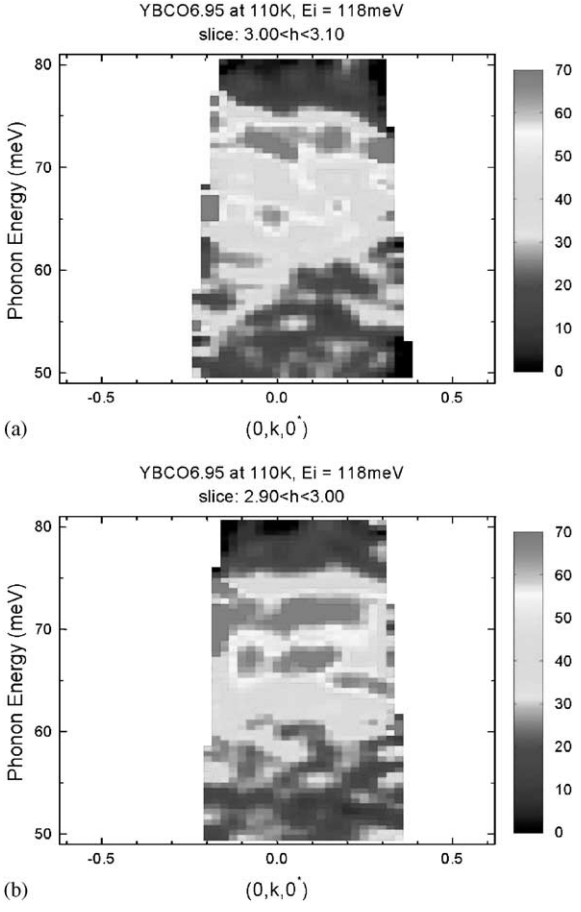

Fig. 3. $S(\boldsymbol{Q}, \omega)$ of $YBa_2Cu_3O_{6.95}$ at $T = 110$ K cut at $h = 3.05$ (a) and 2.95 (b). The TO mode with polarization along a is seen at 72 meV with little dispersion. The TO mode with the polarization along b is seen in (b) with dispersion.

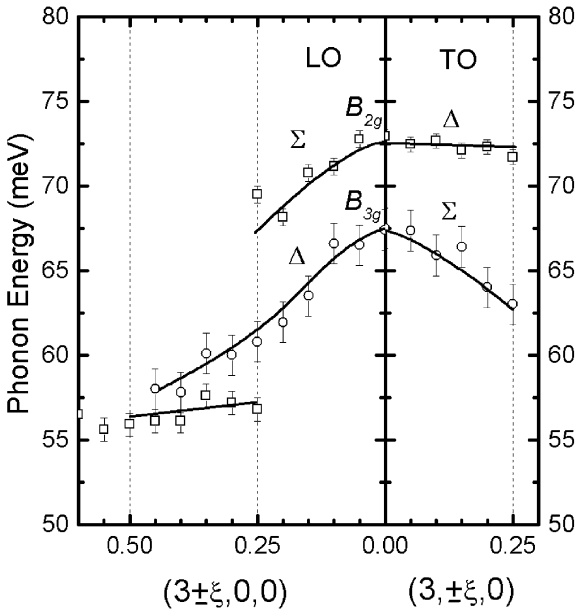

Fig. 4. Phonon dispersion of the Cu–O bond-stretching modes. The LO branches were determined by the k-cut (Fig. 2), the TO branch by the h-cuts (Fig. 3). The mode denoted B_{2g} at the zone center has polarization along a (perpendicular to the chain), while the B_{3g} mode has b-polarization.

b which is parallel to the chain, has a continuous dispersion. However, the other branch, B_{2g} at the zone center and polarization perpendicular to the chain, has a discontinuity at $h = 0.25$, just as was observed for $La_{1.85}Sr_{0.15}CuO_4$ [5]. This jump is consistent with doubling the unit cell in the a-direction [5]. Also the TO and LO are nearly degenerate for the b-polarized branch, suggesting the strong metallic screening in this direction. However, the TO and LO frequencies are different for the a-polarized branch except for $q = 0$. As represented by the Lyddane–Sachs–Teller (LST) relationship, the difference in the LO and TO frequencies arises due to the local Lorentz field created by the dipoles nearby, so it implies dielectric discontinuity across the phonon branch, or imperfect screening of the phonon polarization by electrons. Thus the difference in the dispersion between a- and b-directions indicates strong anisotropy in the dielectric response, and in the underlying electronic structure; metallic along b

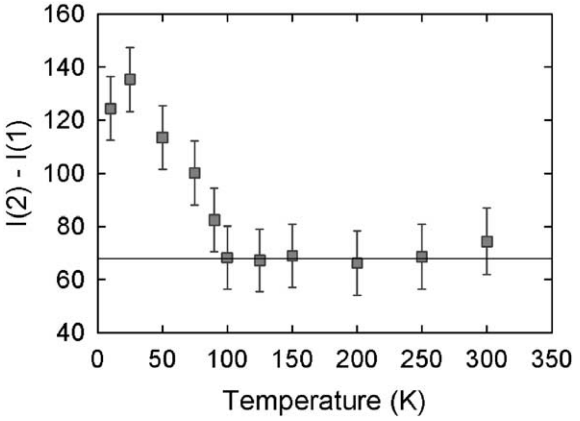

Fig. 5. Temperature dependence of the parameter I_1-I_2 (see text) describing the shift in the phonon intensity. The data has a striking resemblance to the superconductive order parameter ($T_C = 93$ K).

but semi-metallic along a. This anisotropy is consistent with the spin/charge stripe model [6]. In YBCO the stripes appear to be aligned along the b-axis, perhaps pinned by the chain or orthorhombic strain [7], making the whole plane anisotropic. We note here, however, that the standard stripe model assumes the charge periodicity of $4a$ for the optimally doped sample, while the discontinuity in the LO mode observed here and for LSCO suggests the periodicity of $2a$ [5].

At $T = 110$ K the b-polarized LO dispersion is continuous as shown in Fig. 2. At low temperatures, however, the intensity in the middle portion around (0, 0.25, 0) decreased, while the dispersion itself appears to be unchanged. The gapped nature of the a-polarized branch leaks out to the b-polarized branch below T_C. As the parameter to describe this shift we chose the intensities I_1 and I_2 as the average intensity from 51 to 55 meV and from 56 to 68 meV, respectively, at (3.25, 0, 0). Fig. 5 shows $I_1 - I_2$ as a function of temperature. The data were taken with the triple-axis-spectrometer at the HFIR. It is evident that the change is closely related to superconductivity. The crossover of the dispersion gap from 1- to 2-D at T_C may be related to the fact that superconductivity cannot exist in one dimension, reinforcing our suspicion that the dispersion gap may be relevant to the HTSC mechanism.

3. Electron–phonon coupling in the cuprates

The results of the neutron scattering measurement shown above suggest strong anisotropy in the electronic response of the CuO_2 plane. In particular they revealed the semi-metallic nature of the CuO_2 plane in the a-direction. This implies that long-range polar interaction, which is screened in a metal, may play a role in the cuprates, adding another reason to suspect that the electron–phonon interaction in the cuprates may be strong and very different from that in the regular BCS superconductors. In terms of the stripe model this means that the lateral fluctuation of the charge stripe is slow, comparable to phonons in frequency, and does not completely screen the phonon vibration. In comparison charges flow freely along the stripe as in a metal.

Moreover we should note that for the a-polarized branch the TO frequency is *higher* than the LO frequency for $q \neq 0$, while the LO and TO modes are degenerate for both branches at $q = 0$, consistent with the DC metallic behavior. This is a rather unusual phenomenon in the light of the LST relationship. In insulators usually the LO frequency is higher than the TO frequency. The observed inverted LST behavior suggests that the electronic dielectric constant in this frequency range must be negative. Such a situation can occur by electronic anti-resonant overscreening, as was proposed a long ago by Tachiki and Takahashi [8]. In their picture phonons and electrons are in resonance with some phase-shift, forming the vibronic state, e.g. Ref. [9]. Only the phonons with $q > k_F$, the Fermi momentum, will be overscreened, lowering their energy. Thus the dispersion will have a large jump at k_F, just as observed here for the a-polarized phonons. This implies $k_F = 0.25$, consistent with the CDW with the periodicity $2a$. Indeed the ARPES result [10] shows k_F at halfway between X and Γ points. Then the high-energy branch (68–72 meV), from $h = 0$ to 0.25, is not strongly interacting with electrons, while the low-energy branch (~ 55 meV),

from $h = 0.25$ to 0.5, is strongly interacting with electrons, forming the vibronic state. This picture is supported by our earlier observation that the intensity of the low-energy branch is increased with doping [3]. The phonon resonance was assumed in the two-band model of Bussmann–Holder which has many common elements with the Tachiki model [11].

There is some evidence of anti-resonance in the optical data. A notch was observed in the in-plane optical conductivity of YBCO at $435\,\mathrm{cm}^{-1}$ ($=54$ meV, almost exactly the energy of the LO phonon near the zone-edge), first by Orenstein et al. [12] and by many others since then [13–16]. While the conductivity measured by optical reflectivity is for $q = 0$ where metallicity remains, this notch must be indicative of anti-resonance in the system around 55 meV, which is exactly the frequency of the LO phonons at the zone-edge where strong interaction is expected [1]. Also a recent angle-resolved photoemission (ARPES) measurement [17] provides another reason to believe that the electron–phonon interaction is strong for the low-energy branch. The electron dispersion has a kink near the Fermi level, reflecting strong interaction with some quasi-particle. Comparison of the kink energies of a large number of compounds shows that the kink energy is not related to the energies of a superconductive gap, pseudo-gap, or magnetic resonance, but stays always in the range of 50–70 meV, corresponding to the energy of the LO phonons near the zone-edge.

An interesting issue is the direction of the supercurrent. If the vibronic resonance along the *a*-direction is the mechanism of superconductivity, it would result in the $d + s$ symmetry and the supercurrent should be mainly *perpendicular* to the stripes. Indeed the ARPES result [10] appears to show a higher supercurrent density along ***a*** and support this view, although the ARPES result is clouded by the surface states and self-conflicting since the gap seems to be larger in the *b*-direction. Since many stripe theories assume the direction of the stripes to be the superconducting direction e.g. Ref. [18], while others assume perpendicular direction [19,20], this is an important point to be resolved.

4. Conclusions

While the majority of theoreticians in the field of HTSC still assume that phonons are irrelevant to HTSC, recent experimental results are beginning to point to an opposite conclusion. The results of our phonon measurement discussed here strongly challenge the conventional view and suggest that the possibility of phonon involvement in HTSC has to be taken very seriously. We see it as a matter of time when the weight of the experimental evidence changes the majority's view on this matter.

Acknowledgements

The authors are grateful to M. Tachiki, S. Sachdev and J.C. Phillips for useful discussions. The work was supported by the National Science Foundation through DMR96-28134 and DMR01-02565.

References

[1] S. Ishihara, T. Egami, M. Tachiki, Phys. Rev. B 55 (1997) 3163.
[2] R.J. McQueeney, T. Egami, J.-H. Chung, Y. Petrov, M. Yethiraj, M. Arai, Y. Inamura, Y. Endoh, C. Frost, F. Dogan, cond-mat/0105593.
[3] Y. Petrov, T. Egami, R.J. McQueeney, M. Yethiraj, H.A. Mook, F. Dogan, cond-mat/0003414.
[4] K.F. McCarty, et al., Phys. Rev. B 41 (1990) 8792.
[5] R.J. McQueeney, Y. Petrov, T. Egami, M. Yethiraj, G. Shirane, Y. Endoh, Phys. Rev. Lett. 82 (1999) 628.
[6] J.M. Tranquada, et al., Nature (London) 375 (1995) 561.
[7] H.A. Mook, et al., Nature (London) 404 (2000) 729.
[8] M. Tachiki, S. Takahashi, Phys. Rev. B 38 (1988) 218; M. Tachiki, S. Takahashi, Phys. Rev. B 39 (1989) 293.
[9] J.B. Goodenough, J.-S. Zhou, in: A. Bianconi, N.L. Saini (Eds.), Stripes and Related Phenomena, Kluwer Academic/Plenum Publishers, New York, 2000, p. 199.
[10] D.H. Lu, et al., Phys. Rev. Lett. 86 (2001) 4370.
[11] A. Bussmann-Holder, et al., J. Phys. : Condens. Matter 13 (2001) L169.
[12] J. Orenstein, G.A. Thomas, A.J. Millis, S.L. Cooper, D.H. Rapkine, T. Timusk, L.F. Schneemeyer, J.V. Waszczak, Phys. Rev. B 42 (1990) 6342.
[13] G.A. Thomas, M. Capizzi, J. Orenstein, D.H. Rapkine, L.F. Schneemeyer, J.V. Waszczak, A.J. Millis, R.N. Bhatt, Jpn. J. Appl. Phys. Supp. 26 (1987) 2044.

[14] T. Timusk, D.A. Bonn, J.E. Greedan, C.V. Stager, J.D. Garrett, A.H. O'Reilly, M. Reedyk, K. Kamaras, C.D. Porter, S.L. Herr, D.B. Tanner, Physica C 153–155 (1988) 1744.
[15] R.T. Collins, Z. Schlesinger, F. Holtzberg, C. Field, Phys. Rev. Lett. 63 (1989) 422.
[16] D.N. Basov, R. Liang, B. Dabrowski, D.A. Bonn, W.N. Hardy, T. Timusk, Phys. Rev. Lett. 77 (1996) 4090.
[17] A. Lanzara, et al., Nature (London) 412 (2001) 510.
[18] S.A. Kivelson, E. Fradkin, V.J. Emery, Nature (London) 393 (1998) 550.
[19] A.H. Castro-Neto, J. Superconductivity 13, 913 (2000); cond-mat/0102281.
[20] K. Park, S. Sachdev, cond-mat/0104519.